Optical Materials 99 (2020) 109529

Contents lists available at ScienceDirect

Optical Materials

journal homepage: http://www.elsevier.com/locate/optmat

Structural and electronic properties of β-$NaYF_4$ and β-$NaYF_4$:Ce^{3+}

A. Platonenko *, A.I. Popov

Institute of Solid State Physics, Kengaraga st. 8, LV-1063, Riga, Latvia

ARTICLE INFO

Keywords:
ab initio
Defects
Doping
Rare earth luminescencer

ABSTRACT

In this work, the density functional theory approach with linear combination of atomic orbitals (LCAO) as implemented in the CRYSTAL17 computer code is applied to hexagonal β-$NaYF_4$, located in three possible space groups of this compound: $P\bar{6}$, $P6_3/m$ and $P\bar{6}\,2m$. First, the disordered crystalline structure of $NaYF_4$ was modelled in a large supercell containing 108 atoms. In order to obtain better agreement with the experimental data, we used several different exchange-correlation functionals. Basic properties, such as lattice constant, band gap and total energies were calculated and compared for all three space groups and three exchange-correlation functionals - HSE06, PWGGA and PWGGA+13%HF. It was found that for all three functionals, the minimum of total energy corresponds to $P\bar{6}$ space group. Secondly, in order to study the effects associated with the Ce^{3+} impurity and the F center (radiation defect), the $P\bar{6}$ β-$NaYF_4$ structure with the F center and Ce^{3+} or with both was carefully modelled. Taking into account that fluorine atoms have different nearest neighbours, several types of fluorine vacancies were simulated and an appropriate formation energies were determined. Finally, the effects of Ce^{3+} ion substitution of Y ions in different positions as well as formation of Ce^{3+}, the F center defect pairs were also studied and an appropriate incorporation energies were calculated.

1. Introduction

The sodium yttrium fluoride $NaYF_4$ [1–5] together with similar fluorides, such as $LiYF_4$, $LiLuF_4$, $NaGdF_4$ and etc. [2,6,7], belongs to the family of metal fluorides $MREF_4$ (M = alkali or alkali earth metal, RE = Ln^{3+} rare earth ion), which have been successfully grown as single crystals or synthesized as nano and micro-materials through different methods.

When these materials are doped with one or two rare-earth ions (Eu^{3+}, Eu^{2+}, Dy^{3+}, Tb^{3+}, Ce^{3+}, Sm^{3+}), which are considered to be excellent luminescence activators, they often exhibit unique and outstanding optical and luminescent properties, thereby receiving tremendous attention due to their potential application in a variety of different modern disciplines, such as full color displays, scintillators, noncontact fluorescence thermometers, drug delivery, security inks and etc [1–7 and references therein]. Among all lanthanide ions, Ce ions are the most widely used as the emitting species in many traditional phosphors [8–14]. In the case of $NaYF_4$, the dopant effects on particle morphology and optical properties have been also reported in Refs. [15–18].

According to Chong et al. [19], the experimental band gap edge of $NaYF_4$ is of 8 eV, so this material belongs to the class of wide band gap fluorides. This value is in good agreement with recent findings [20,21]. Fundamental view of the electronic structure β-$NaYF_4$, β-$NaGdF_4$, and β-$NaLuF_4$ was presented in Ref. [21], however, the effects of Ce-doping and the F center formation have not been yet considered.

It is well known that the F center (fluorine vacancy with one trapped electron) is the main and simplest radiation defect in wide-band gap fluorides, including alkaline-earth fluorides (CaF_2, BaF_2, SrF_2 and MgF_2) and some perovskites ($KMgF_3$, $BaLiF_3$, $RbMgF_3$, $CaRbF_3$). The basic properties of the F-type centers in these materials were reviewed [22,23]. The F centers were also found in $LiYF_4$ and $LuLiF_4$ [24]. Furthermore, it was reported that impurity doping has a strong effect to diminish the F center concentration.

It is important to note that in many cases, the F centers are created near impurity, to form the so called F_A centers, such as F_A(Li) or F_A (Tl) in KCl [25]. The localization of an electron either on an impurity or on a vacancy strongly determines, for example, its laser-active properties. The F centers located near hole impurity centers, for example the F centers in BaFBr:Eu, CsBr:Eu, KBr:In and many others) are very important for radiation image recording in industry and medical diagnostics [26,27].

In the present paper, we performed the state-of-the-art *ab initio electronic and atomic structure calculations* for pure and Ce-doped $NaYF_4$

* Corresponding author.
E-mail address: a.platonenko@cfi.lu.lv (A. Platonenko).

https://doi.org/10.1016/j.optmat.2019.109529
Received 31 December 2018; Received in revised form 5 November 2019; Accepted 10 November 2019
Available online 10 December 2019

Table 1
Properties of hexagonal $NaYF_4$ within different space groups calculated by different Hamiltonians. Total energy difference is given with respect to a supercell with a lowest energy.

Hamiltonian	HSE06			PWGGA			PWGGA +13% HF		
Space group	$P\bar{6}$	$P6_3/m$	$P\bar{6}2\,m$	$P\bar{6}$	$P6_3/m$	$P\bar{6}2\,m$	$P\bar{6}$	$P6_3/m$	$P\bar{6}2\,m$
ΔTotal. Energy, eV	0.00	0.65	1.27	0.00	0.60	1.15	0.00	0.63	1.22
E_g, eV	9.61	9.13	9.13	7.28	6.80	6.84	9.06	8.39	8.43
a, Å	5.988	5.983	5.988	6.038	6.066	6.039	6.005	6.035	6.008
c, Å	3.595	3.594	3.595	3.612	3.605	3.616	3.600	3.593	3.602

crystals. Taking into account that the F-centers are the simplest radiation defects, which are produced in this and other similar materials, and which determine the radiation hardness of the most oxide and halide scintillator materials, we also calculated their electronic structure. As the result, the electronic and atomic structure of pure $NaYF_4$ crystals are presented and discussed. In addition, we have also calculated the Raman vibrational spectra for different $NaYF_4$ phases and compared them with available experimental data. In the case of Ce-doped models, we have analyzed various positions for substitution, compared incorporation energies and the electronic structures for substitutions of Y atoms at 1a and 1f Wyckoff positions.

Finally, we considered the F centers in $NaYF_4$ and determined their formation energies and the energy level position within the band gap.

2. Computational details

All simulations have been performed within the periodic model using method of the linear combination of atomic orbitals (LCAO) based on Density Functional Theory (DFT) methodology as implemented in the CRYSTAL17 computer code [28]. We have used the full-electron basis set (BS) of atomic Gaussian Type Functions (GTFs) for Na and F atoms: 8*s*-511*sp* for Na [29], and 7*s*-311*sp* for F [30] respectively. For heavy atoms the basis sets with effective core potentials have been used: 31*sp*-2*d* basis set with ECP implemented by Hay and Wadt for Y atoms [31], and ECP 4321*sp*-61*d*-431*f* basis set by Meyer for Ce atoms [32]. The reciprocal space integration has been performed by sampling the Brillouin zone with the $4 \times 4 \times 4$ Monkhorst-Pack mesh [33] for 108 atoms supercell. Convergence criteria was set to 10^{-7} a.u. for self-consistency procedure. The F-center was simulated by removing electrons and nuclear charge from the missing fluorine atom site (F atom removed), leaving the basis set centered at the atomic position. Calculations of point defects were performed using the standard geometry optimization and energy minimization procedures [28]. For phonon calculations, we use harmonic approach and the direct frozen phonon method realized in the CRYSTAL17 code [34], with SCF convergence set to 10^{-9} a.u.. The relative Raman vibrational intensities are computed analytically by exploiting the scheme illustrated in Ref. [35]. It is based on the solutions of first- and second-order Coupled-Perturbed-Hartree-Fock/Kohn-Sham (CPHF/KS) equations.

Three exchange-correlation functionals were tested to obtain best description of the structural and electronic properties of β-$NaYF_4$: HSE06 [36], PWGGA [37] and PWGGA with 13% added non-local Hartree-Fock exchange part.

3. Results and discussion

3.1. Model of disordered β-$NaYF_4$

The crystalline structure of hexagonal $NaYF_4$ has a specific disorder. Some of the positions could be occupied by Na or Y atoms. Literature data has reported three different possible space groups for describing β-$NaYF_4$ structure: $P\bar{6}$, $P\bar{6}\ 2\,m$ and $P6_3/m$. To reproduce disordered structure and simulate different atom arrangement in different space groups, three types of $2 \times 2 \times 3$ supercells were constructed following [38]. In this work, *ab initio* molecular dynamics was used to evaluate stability of different space groups. Here we use proposed structures for a full geometry optimization without constraints using previously mentioned Hamiltonians. Total energies of supercells, cell parameters and band gaps (Table 1) were compared, to find a model and computational scheme which gives better agreement with available experimental data.

For our further calculations, we choose PWGGA+13%HF exchange-correlation functional and $P\bar{6}$ space group as a lowest energy configuration. It gives reasonable, slightly overestimated band gap (experimental value ~8 eV) and good agreement on lattice parameters (exp. a = 5.96 Å and c = 3.53 Å [39]). From Table 1 we can see a pattern, where calculated band gaps for $P\bar{6}\ 2\,m$ and $P6_3/m$ models are consistently smaller for all Hamiltonians. Calculated Partial Density of States (PDOS) for each model (Fig. 1) show that valence band fully consists of 2*p* fluorine orbitals, while conduction band is made of F 3*s* orbitals and Y 4*d*5*s* orbitals. The gap between highest core band and valence band is about 11 eV, what is larger than calculated band gap. Thus, cross-luminescence mechanism is forbidden in pure $NaYF_4$, but defects and dopants could create additional levels in the gap, making more possibilities for this material to serve as a scintillator. The main differences in DOS of different models are due to Na 2p orbitals, which is a result of different Na surrounding, while core-valence gap and valence bandwidth is similar in all cases.

In $P\bar{6}$ (Fig. 2) structure Y atoms are nine-coordinated on both 1a and 1f Wyckoff positions, while Na atoms are seven-coordinated. Fluorine

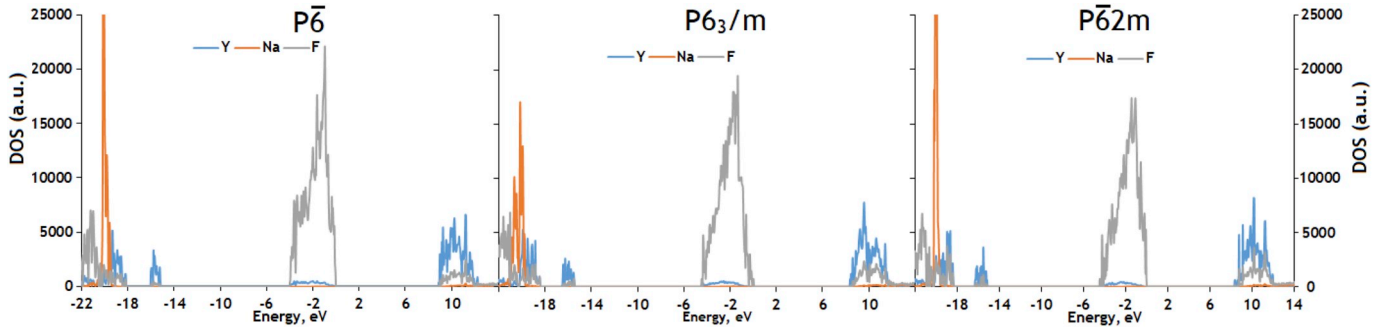

Fig. 1. Partial Density of States of three calculated space groups of $NaYF_4$. Zero energy corresponds to highest occupied energy level.

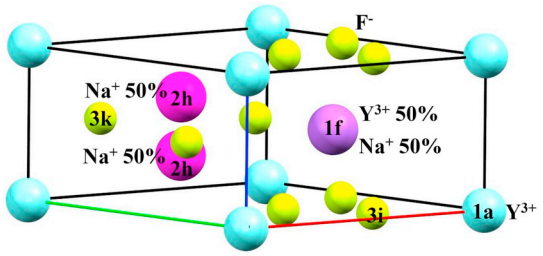

Fig. 2. Crystal structure of β-$NaYF_4$, space group $P\bar{6}$, Z = 1.5. Figure shows perfect positions before optimization.

atoms are expected to be four-coordinated, but due to disorder some of them have five cations within first nearest neighbours. Radial distribution function (Fig. 3) shows many broad peaks for Na atoms, indicating high variety of Na–F bond lengths. Taking closer look on Na atoms positions in the structure, we can notice that sodium atoms occupying 2 h positions have strong displacements along *z*-axis. Yttrium atoms occupying 1f positions show much less distortion, preserving higher symmetry around the site. In total, structure distortion results in shortening of Y–F bond lengths and increase in Na–F distances.

Calculated phonon modes and the Raman spectra (Fig. 4) for $P\bar{6}$ space group are in good agreement with available experimental data. Fig. 4 also shows the Raman spectra for two other space groups. where all peaks are consistently shifted to smaller energies, as well the relative intensities do not match with experimental spectra. The experimental data reveal three dominant phonon modes 298, 370 and 418 cm^{-1} [40]. Calculated spectra have five dominant modes 292, 310, 332, 369 and 425 cm^{-1}. Taking into account positions and intensities of calculated modes of $P\bar{6}$ space group, the effective phonon energy is estimated ~326 cm^{-1}, whereas the experimentally reported value is ~360 cm^{-1}.

3.2. The F-centers and Ce^{3+} doping in β-$NaYF_4$

Creation of fluorine vacancy in $NaYF_4$ structure results in formation of the F-centers. As was mentioned previously, fluorine atoms have different surrounding and coordination. To evaluate influence of the surrounding on defect properties, four different F-centers were calculated. Formation energies of all studied defects were negligibly small (<0.1 eV). Calculated Density of States showed formation of the F-centers, introduced energy level lies near below conduction band and defects does not introduce any changes to core-valence gap. The excitation energy with respect to the bottom of the conduction band lies between 1.2 eV and 3.2 eV, what is actually the result of lattice disorder.

Doping of hexagonal $NaYF_4$ with trivalent RE ions can result in various positions of dopant. Calculations have been performed for Ce^{3+} substituting yttrium atom on 1a and 1f Wyckoff positions. After obtaining a ground state solution, the F-center was introduced at a site of fluorine atom nearest to cerium ion. The resulting density of state are shown in Fig. 5. The electronic structure of Ce^{3+} ion levels shows that possible f-d transition requires 3.3 eV in 1a position, while at 1f position this energy reduces to 2.7 eV. In previous work, the position of highest occupied Ce^{3+} level was reported at about 2 eV below the bottom of the conduction band [41]. Here we see, that this value also depends on the position and surrounding of dopant ion. Comparing incorporation energies, we found that Y substitution on 1f position is slightly more energetically favourable (~0.1 eV). Introduction of the F-center in both cases results in a new energy level ~1.5 eV above the Ce^{3+} 4f level (Fig. 5). Thus in Ce-doped $NaYF_4$ position of the F-center level is mostly determined by neighboring cerium ion, and not by the lattice disordering. It is important to note, that experimental value for 4f-5d

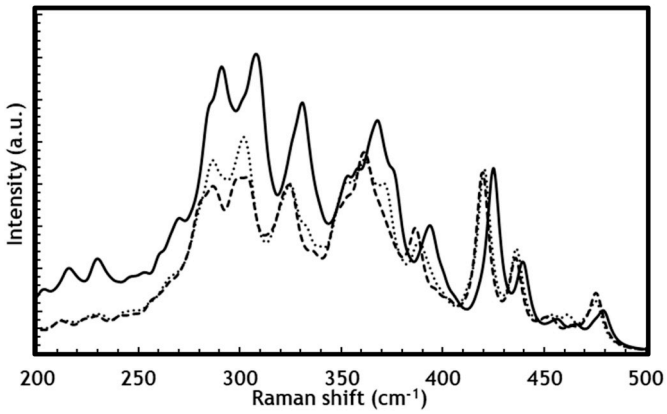

Fig. 4. Calculated Raman spectra for three space groups of $NaYF_4$: $P\bar{6}$ (solid line), $P\bar{6}$ 2 m (dotted line) and $P6_3/m$ (dashed line). All spectra simulated for powder samples at 293 K temperature.

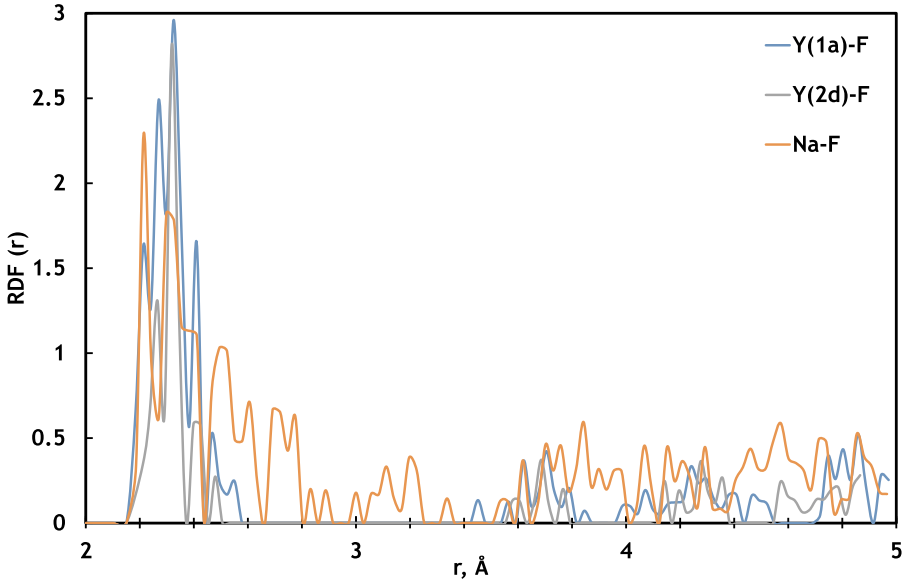

Fig. 3. Joint Radial Distribution Function of Y–F and Na–F contacts in $NaYF_4$ $P\bar{6}$ phase.

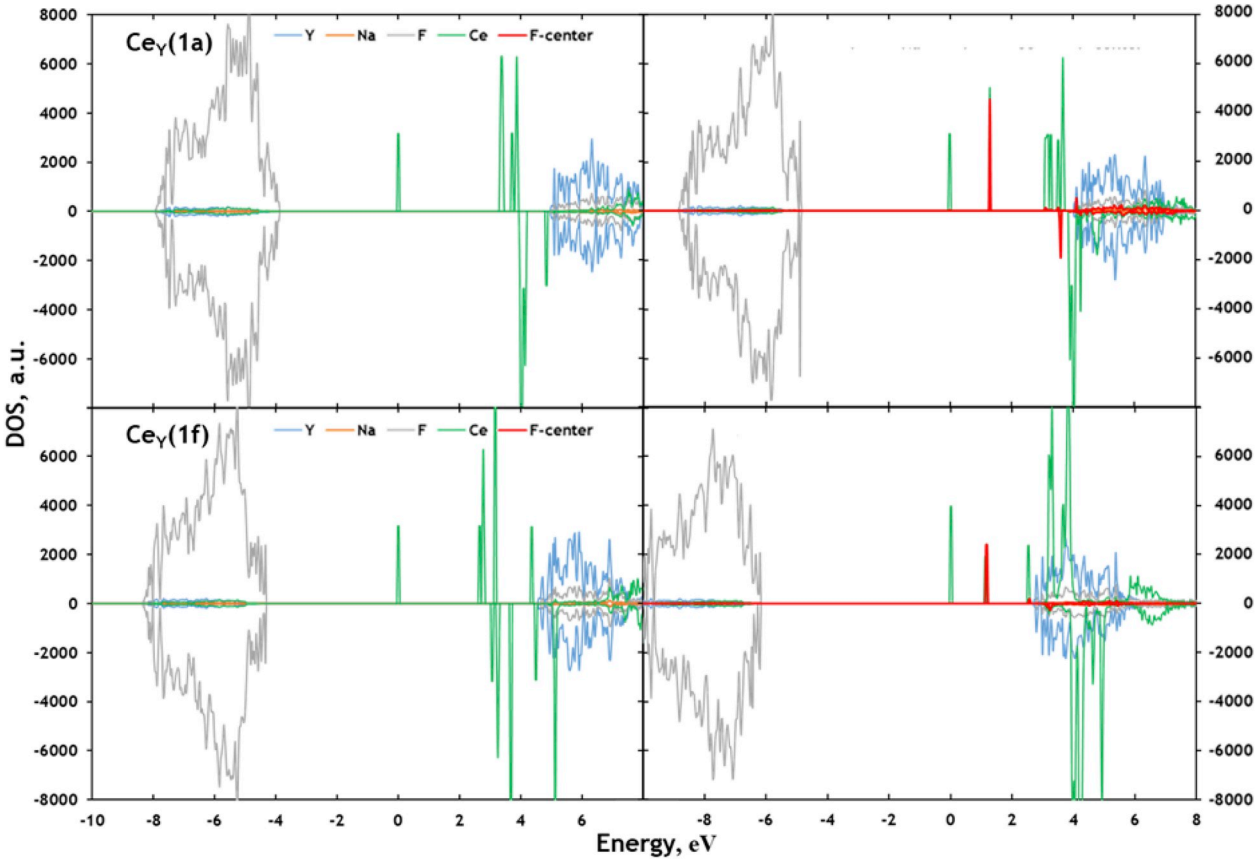

Fig. 5. Partial Density of States of Ce^{3+} doped $NaYF_4$. Top figures correspond to Ce_Y substitution on 1a position, bottom figure - Ce_Y on 1f position. The positive and negative parts represent the spin-up and spin-down states, respectively. The F-center and Ce^{3+} DOS are multiplied 20x. Zero energy corresponds to highest occupied energy level of Ce^{3+} ion. F-centers produce one additional occupied level above the energy level of Ce^{3+} ion.

transition of Ce^{3+} in $NaYF_4$ is about 4.8 eV [42].

4. Conclusions

In summary, disordered structure of β-$NaYF_4$ has been calculated using DFT LCAO approach. The calculated radial distribution functions and Raman spectra were compared with theoretical [38] and experimental data [40], demonstrating very reasonable agreement and supporting hypothesis that β-$NaYF_4$ exist in $P\bar{6}$ space group, where Y sites maintain more fixed Y–F bond lengths, but Na sites have pronounced disorder along the *z*-axis. Modelling of the F-centers and Ce^{3+} doping shows that from the energetics point of view, different Wyckoff positions of Y atoms for Ce doping are more or less equal, however, the electronic structures of defects differ for various lattice sites and this could affect their photoluminescence properties. The position of the F-center energy level in undoped $NaYF_4$ varies between 1.2 and 3.2 eV below the bottom of the conduction band (due to lattice disorder), while in Ce-doped $NaYF_4$ it is more pronounced and located 1.5 eV above the Ce^{3+} 4f level and around 2 eV below the bottom of the conduction band. Finally, we conclude, that for modelling of defects in this kind of materials, the effects of disordering are very important and should be always taken into account, since it affects both electronic and vibrational properties of materials.

Declaration of competing interest

The authors declare that they have no known competing financial interests or personal relationships that could have appeared to influence the work reported in this paper.

Acknowledgement

AP is indebted for a financial support provided by Scientific Research Project grant for Students and Young Researchers Nr. SJZ/2017/3 sponsored at the Institute of Solid State Physics, University of Latvia, while AIP is thankful for the financial support from Latvian Research Council lzp-2018/1-0214.

References

[1] N. Menyuk, K. Dwight, J.W. Pierce, Appl. Phys. Lett. 21 (4) (1972) 159–161.
[2] L. Wang, Y. Li, Chem. Mater. 19 (4) (2007) 727–734.
[3] T.K. Pathak, A. Kumar, L.J.B. Erasmus, H.C. Swart, R.E. Kroon, Spectrochim. Acta 207 (2019) 23–30.
[4] E. Elsts, G. Krieke, U. Rogulis, K. Smits, A. Zolotarjovs, J. Jansons, A. Sarakovskis, K. Kundzins, Opt. Mater. 59 (2016) 130–135.
[5] A. Tuomela, V. Pankratov, A. Sarakovskis, G. Doke, L. Grinberga, S. Vielhauer, M. Huttula, J. Lumin. 179 (2016) 16.
[6] T. Yanagida, Y. Fujimoto, S. Ishizu, K. Fukuda, Opt. Mater. 41 (2015) 36–40.
[7] T. Yanagida, Y. Fujimoto, K. Fukuda, V. Chani, Nucl. Instrum. Methods A 729 (2013) 58–63.
[8] M.V. Anan'ev, E.Kh Kurumchin, G.K. Vdovin, N.M. Bershitskaya, Russ. J. Electrochem. 48 (9) (2012) 871–878.
[9] A.V. Sidorenko, A.J.J. Bos, P. Dorenbos, C.W.E. van Eijk, P.A. Rodnyi, I. V. Berezovskaya, V.P. Dotsenko, A.I. Popov, J. Appl. Phys. 95 (2004) 7898–7902.
[10] A. Lushchik, Ch Lushchik, A.I. Popov, K. Schwartz, E. Shablonin, E. Vasil'chenko, Nucl. Instrum. Methods B 374 (2016) 90.
[11] I.I. Syvorotka, D. Sugak, A. Wierzbicka, A. Wittlin, H. Przybylińska, J. Barzowska, A. Barcz, M. Berkowski, J. Domagala, S. Mahlik, M. Grinberg, J. Lumin. 164 (2015) 31–37.
[12] Y. Zhydachevskyy, I.I. Syvorotka, V. Tsiumra, M. Baran, L. Lipińska, A. Wierzbicka, A. Suchocki, Sol. Energy Mater. Sol. Cells 185 (2018) 240–251.
[13] H. Przybylińska, C.G. Ma, M.G. Brik, M.G. Brik, A. Kamińska, P. Sybilski, A. Wittlin, M. Berkowski, Y. Zorenko, V. Gorbenko, H. Wrzesinski, A. Suchochki, Appl. Phys. Lett. 102 (24) (2013) 241112.

[14] E. Polisadova, D. Valiev, V. Vaganov, V. Oleshko, T. Han, C. Zhang, A. Burachenko, A.I. Popov, Opt. Mater. 96 (2019) 109289.
[15] M. Ding, Y. Li, D. Chen, H. Lu, J. Xi, Z.J. Ji, Alloys and Compd. 658 (2016) 952–960.
[16] P. Ghosh, A. Kar, A. Patra, Nanoscale 2 (7) (2010) 1196–1202.
[17] L.T.K. Giang, L. Marciniak, D. Hreniak, T.K. Anh, L.Q. Minh, J. Electron. Mater. 45 (10) (2016) 4790–4795.
[18] D. Wawrzynczyk, A. Bednarkiewicz, M. Nyk, J. Cichos, M. Karbowiak, D. Hreniak, W. Strek, M. Samoc, J. Nanosci. Nanotechnol. 12 (3) (2012) 1886–1891.
[19] K. Chong, T. Hirai, T. Kawai, S. Hahshimoto, N. Ohno, J. Lumin. 122–123 (2007) 149–151.
[20] G. Yao, Q.G. Meng, M.T. Berry, P.S. May, D.S. Kilin, Mol. Phys. 113 (3–4) (2015) 358.
[21] B. Huang, H. Dong, K.L. Wong, L.D. Sun, C.H. Yan, J. Phys. Chem. C 120 (33) (2016) 18858.
[22] V.M. Lisitsyn, L.A. Lisitsyna, A.I. Popov, E.A. Kotomin, F.U. Abuova, A. Akilbekov, J. Maier, Nucl. Instrum. Methods B 374 (2016) 24.
[23] A.I. Popov, E.A. Kotomin, J. Maier, Nucl. Instrum. Methods B 268 (19) (2010) 3084–3089.
[24] A. Bensalah, M. Nikl, A. Vedda, K. Shimamura, T. Satonaga, H. Sato, T.Fukuda, G. Boulon radical effect def, Sol. 157 (2002) 563–567.
[25] S.V. Nistor, D. Schoemaker, I. Ursu, Phys. Status Solidi B 185 (1994) 9.
[26] S. Schweizer, Phys. Status Solidi A 187 (2001) 335–393.
[27] A.I. Popov, J. Zimmermann, G.J. McIntyre, C. Wilkinson, Opt. Mater. 59 (2016) 83–86.
[28] R. Dovesi, A. Erba, R. Orlando, C.M. Zicovich-Wilson, F. Pascale, B. Civalleri, K. Doll, N.M. Harrison, I.J. Bush, P. D'Arco, M. Llunell, M. Causà, Y. Noël, L. Maschio, M. Rerat, S. Casassa, CRYSTAL17, CRYSTAL17 User's Manual, University of Torino, Torino, 2017.
[29] R. Dovesi, C. Roetti, C. Freyria Fava, M. Prencipe, V.R. Saunders, Chem. Phys. 156 (1991) 11–19.
[30] R. Nada, C.R.A. Catlow, C. Pisani, R. Orlando, Model. Simul. Mater. Sci. Eng. 1 (1993) 165–187.
[31] P.J. Hay, W.R. Wadt, J. Chem. Phys. 82 (1985) 284.
[32] J. Graciani, A.M. Marquez, J.J. Plata, Y. Ortega, N.C. Hernandez, A. Meyer, C. M. Zicovich-Wilson, J.F. Sanz, J. Chem. Theory Comput. 7 (2011) 56–65.
[33] H.J. Monkhorst, J.D. Pack, Phys. Rev. B 13 (1976) 5188–5192.
[34] F. Pascale, C.M. Zicovich-Wilson, F. Lopez Gejo, B. Civalleri, R. Orlando, R. Dovesi, J. Comput, Chem. 25 (2004) 888–897.
[35] L. Maschio, B. Kirtman, R. Orlando, M. Rérat, R. Dovesi, J. Chem, Phys 139 (16) (2013), 164101.
[36] J.P. Perdew, K. Burke, M. Ernzerhof, Phys. Rev. Lett. 77 (1996) 3865–3868.
[37] J.P. Perdew, Wang Yue, Phys. Rev. B 33 (1986) 8800–8802.
[38] B. Szefczyk, R. Roszak, S. Roszak, RSC Adv. 4 (2014) 22526.
[39] A. Grzechnik, P. Bouvier, M. Mezouar, M.D. Mathews, A.K. Tyagi, J. Köhler, J. Solid State Chem. 165 (2002) 159–164.
[40] J.F. Suyver, J. Grimm, M.K. van Veen, D. Biner, K.W. Kramer, H.U. Gudel, J. Lumin. 117 (2006) 1–12.
[41] G. Yao, Q. Meng, M.T. Berry, P.S. May, D.S. Kilin, Mol. Phys. 113 (2014) 385–391.
[42] P. Gnosh, A. Kar, A. Patra, Nanoscale 2 (2010) 1196–1202.

Institute of Solid State Physics, University of Latvia as the Center of Excellence has received funding from the European Union's Horizon 2020 Framework Programme H2020-WIDESPREAD-01-2016-2017-TeamingPhase2 under grant agreement No. 739508, project CAMART²